Ready-to-be-addressed oxo-clusters: individualized, periodically organized and separated from the substrate

Juba Salhi, Jan Patrick Calupitan, Michele Mattera, David Montero, Antoine Miche, Régina Maruchenko, Anna Proust, Guillaume Izzet, David Kreher, Imad Arfaoui, et al.

Ready-to-be-addressed oxo-clusters: individualized, periodically organized and separated from the substrate

Juba Salhi,a Jan Patrick Calupitan,a Michele Mattera,a David Montero,b Antoine Miche,c Régina Maruchenko,a Anna Proust,a Guillaume Izzet,a David Kreher,d Imad Arfaoui,e Florence Volatron*a

Clusters and oxo-clusters are drawing attention for their amazing physical properties, especially at the scale of the single molecule. However, chemical methods to organize them individually on a surface are still lacking. In this study we show that it is possible to periodically organize individual polyoxometalates thanks to their ordering by a new supramolecular assembly.

Controlled organization of single molecules on surfaces, i.e. isolating molecules at the nanoscopic scale, remains a great challenge nowadays, especially for clusters and metal-oxygen clusters.1–6 In nanoelectronics and nanospintronics, the functional molecules, which play the role of a molecular electronic component, have to satisfy particular conditions : i) to be isolated from each other, to preserve individual properties ;7–10 ii) to be separated from the substrate which could potentially influence the physical properties of the functional molecule, even leading in some cases to the disappearance of the molecular property ;11–16 iii) to be periodically organized on a substrate so that they could be addressed easily. Among oxo-clusters, polyoxometalates (POMs), made of early transition metals in their highest oxidation state (WVI, MoVI, …), occupy an increasingly important place in the field of molecular electronics and spintronics, due to their remarkable redox, photoredox and magnetic properties.17–21 In the last two decades, strong efforts were devoted to their processing in thin films and monolayers,22–27 or as individual molecules, trapped in break-junction set-ups or randomly stuck on substrate defects.2,12,28,29 To ensure a periodic and individualized organization of the molecules, an elegant and promising approach takes advantage of the templating effect of a bidimensional (2D) supramolecular assembly on a substrate.30–32 Two previous attempts described in the literature used the pores of a porous molecular network or co-assembled POMs with self-assembling molecules, but failed to individualize the POMs (several POMs localized in molecular pores) or to thoroughly characterize the co-assembly.33,34

In this communication, we report the first POMs properly individualized, organized and separated from the substrate. The strategy consists in using a new 2D supramolecular assembly on highly-oriented pyrolytic graphite (HOPG), similar to the previously widely studied 1,3,5-tris[(E)-2-(3,5-didodecyloxyphenyl)-ethynyl]-benzene molecule (denoted hereafter TSB-C12)35 but with a triazine core (the 2,4,6-tris[(E)-2-(3,5-didodecyloxyphenyl)-ethynyl]-s-triazine, denoted as Tz-C12). Its protonation should allow the deposition of [PMo12O40]3- by electrostatic interaction (Scheme 1), a widely used technique for the elaboration of POMs monolayers and thin films.36,37 Moreover, addition of the acidic salt H3[PMo12O40] should ensure the simultaneous acidification of the triazine core and POMs deposition. In the case of highly charged molecules as POMs, this method of deposition is crucial as it allows to counter the cation driven POM-to-POM electrostatic interactions that often promote their aggregation.

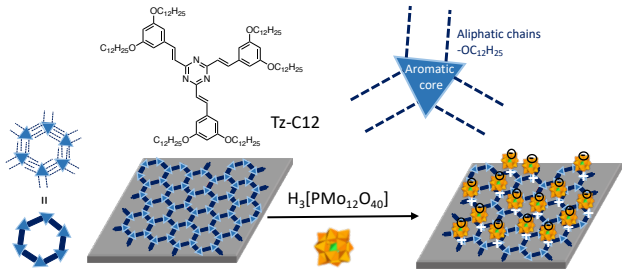

Scheme 1. The Tz-C12 molecule and the strategy of deposition of oxo-clusters on self-assembled Tz-C12 on HOPG in a honeycomb arrangement.

In the supramolecular assembly, the triazine cores should be spaced by 2 nm from each other (see Figure S1), which should allow a regular spatial distribution of the positive charges on the surface and thus individualize the deposited POMs. Moreover, in this case the POMs should be deposited on the backbone of the supramolecular network and not in the pores, restricting direct interaction with the substrate, thereby avoiding pore-filling schemes that might require supplementary synthesis steps.38–40 To prove unambiguously the homogeneous and periodic organization of the POMs, various characterizations were performed at different scales. Macroscale deposition of the POMs directed by electrostatic interactions on the protonated triazine core was first confirmed by X-ray photoemission spectroscopy (XPS). To unambiguously prove the long-range microscale organization of the POMs, we performed field emission scanning electronic microscopy (FESEM), Energy dispersive X-ray spectrometry (EDS), and atomic force microscopy (AFM). At the nanoscale, the periodic and individualized POMs were imaged by scanning tunneling microscopy (STM).

Tz-C12 was synthesized by condensation under basic conditions of 2,4,6-trimethyl-s-triazine, prepared by trimerization of ethyl acetimidate,41 and 3,5-(tridecyloxy)benzaldehyde, prepared by a Williamson reaction, and obtained as a white powder after flash chromatography with a global yield of 55% (see the Supporting Information for synthetic details).42 The molecule was characterized by 1H and 13C NMR spectroscopy, as well as mass spectrometry (Figures S2 and S3). DFT calculations were also performed to attribute unambiguously the two doublets on the 1H spectrum corresponding to the two ethylenic protons (Figures S6 and S7). As the pKa of the triazine is known to be very low in water, we first checked the possibility to protonate the molecule in solution, in an organic media, before experiments on surface. Thus, the stepwise addition of trifluoroacetic acid (TFA) to a solution of Tz-C12 in chloroform was followed by NMR and UV-visible spectroscopies. The NMR spectrum (Figure S4) showed respective downfield shifts of the two ethylenic protons upon addition of TFA, indicative of less electronic density on these sites which could be attributed to the protonation of at least one triazine ‘s nitrogen atom. UV-visible spectroscopy allowed to prove that the second protonation could be reached, thanks to the successive appearance of isosbestic points as the acid was added (Figure S5). These preliminary studies therefore proved that the triazine core could be protonated in organic media in the presence of TFA, promising for the assembly scheme illustrated on Scheme 1. The self-assembling properties of the Tz-C12 were finally studied: a highly diluted solution of Tz-C12 (5.10-5 M in toluene) was drop-casted on HOPG and characterized by STM (denoted hereafter Tz-C12 sample). The organization of the Tz-C12 was very similar to that of the TSB-C12 molecules with the concomitance of areas with hexagonal and herringbones arrangements (Figure S8).43

Then, we proceeded on depositing the POMs on the pre-assembled array of TzC12 on HOPG. Once the TzC12 was drop-deposited on HOPG and the solvent dried, the Tz-C12 sample was dip-coated in a 1mM solution of H3[PMo12O40] in acetonitrile, then slowly removed from the solution to avoid excess of material on the substrate and the formation of aggregates (denoted hereafter Tz-C12-POM sample).

XPS allowed the chemical analysis of the surface at a wide scale and the determination of the triazine cores acidification rate thanks to the ammonium peak at the nitrogen core level. To avoid any interaction with water molecules in air that could contribute to this ammonium peak by the formation of hydrogen bonds,44 the deposition of Tz-C12 and POMs was done under inert atmosphere in anhydrous solvents (see Supporting Information for experimental details). The N 1s spectrum of Tz-C12 self-assembled on HOPG showed one single peak at 398.5 eV, corresponding to nitrogen atoms of the triazine cores (Figure 1a). When the sample was immersed in the POMs solution, a second peak appeared at around 400.9 eV, typical of protonated nitrogen atoms (Figure 1b). With the triazine core protonated and thus positively-charged, it must require a counter-anion, i.e. H2[PMo12O40]-. This was confirmed by the presence of molybdenum at 232.8 eV and 235.9 eV corresponding to the 3d5/2 and 3d3/2 levels of Mo(VI) ions linked to oxygen atoms (Figure 1c).24 Phosphorus was also present as a wide and hardly exploitable peak as usually obtained for POMs deposited on surfaces (Figure S9).24 From Figure 1b, around 20% of the nitrogen atoms on the surface were protonated, which means that around two thirds of the Tz-C12 molecules were protonated upon 2D-assembly on HOPG, conferring it a positive charge which could be exploited towards attractive electrostatic interactions with the deprotonated POM counter-anion H2P[Mo12O40]-. To further confirm the presence of POMs on the substrate, FESEM and EDS characterizations were performed. We based our argument on molybdenum signature in the Tz-C12-POM sample.

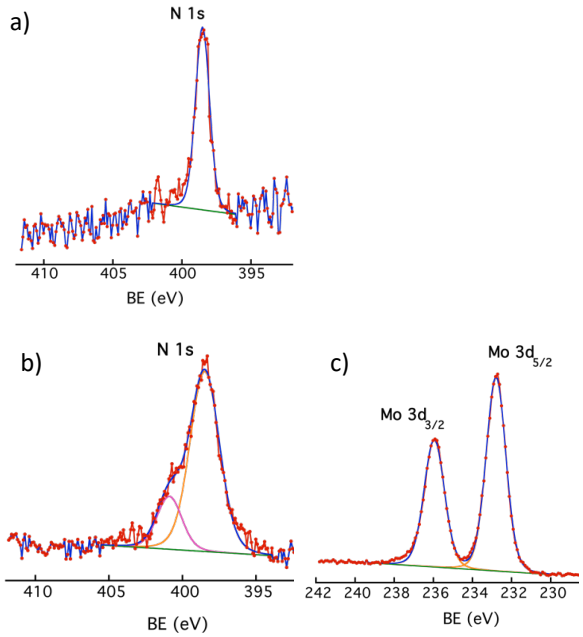

Figure 1. High resolution XPS spectra of a) the Tz-C12 sample at the N 1s core level; b) the Tz-C12-POM sample at the N 1s core level and c) Mo 3d core level.

First, the SEM imaging at normal incidence (0°) showed the aspect of the film after POMs deposition: it appeared very thin and quite homogeneous, as the film formed by the pristine Tz-C12 layer (Figure 2a-b). No aggregates were found on the whole 1x1 cm2 substrate. Our POM deposition was equivalent to a very thin film of molybdenum on the surface from an EDS analytic perspective, yet SEM-EDS had a large bulk analysis volume. In order to selectively analyze the surface, measurements were done at a grazing angle (85° from the normal) to decrease electron penetration (Figure 2c). This revealed a molybdenum peak (Figure 2d), which when quantified, reached an average of 0.6% by weight molybdenum; the rest was mainly the carbon substrate (Figure S10). Interestingly, on a blank sample

made of the self-assembled TSB-C12 molecule (without the triazine core and thus not being able to be protonated) and although immersed in the solution of POM, no molybdenum could be detected with the same setup (Figure S11). The deposition of the POMs by electrostatic interactions on the Tz-C12 self-assembled on HOPG was thus undoubtedly confirmed by cross-checking the observations and information gathered by the XPS and FESEM/EDS techniques.

To gain more insight about the distribution of the POMs on the surface at the microscale, we performed Atomic Force Microscopy (AFM) measurements. The AFM images of the Tz-C12-POM sample were very similar to the FESEM images. Interestingly, the analysis of the AFM images allowed to demonstrate qualitatively a large coverage rate of the assumed POMs films (Figure 3b), in good agreement with the large protonation rate calculated from the XPS data. Moreover, these films seem to be made up of a finely structured network, which could be interpreted as well-organized POM arrays inside these films (see Figure S12). The thickness of the films was about 3 nm, that can reasonably match the thickness of one layer of POMs, on the top of Tz-C12 layer (Figure 3).

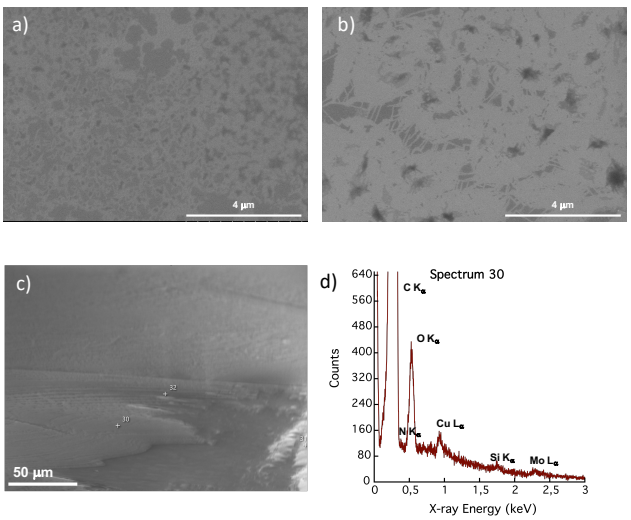

Figure 2. FESEM images at 0° tilt (normal incidence) of a) the Tz-C12 sample (white contrast corresponds to the Tz-C12 layer) and b) the Tz-C12-POM sample (white contrast corresponds to the POMs layer); c) FESEM image at 85° tilt of the Tz-C12-POM sample; d) EDS spectrum at 85° tilt of the Tz-C12-POM sample showing the presence of molybdenum. More details on the weight percentages can be found in the Supplementary Information.

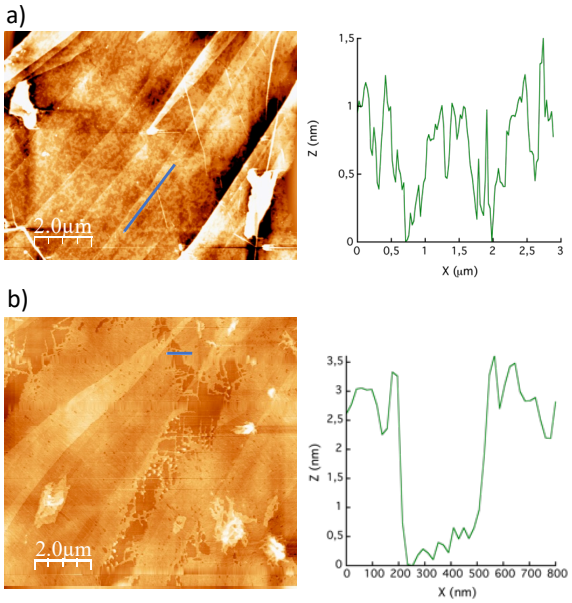

Figure 3. AFM image and heigh profile of a) the Tz-C12 sample showing the presence of a flat film of ~ 1 nm thickness, b) the Tz-C12-POM sample.

It is worth noting here that all AFM experiments were repeated several times at different spots, and the results of morphological features observed on Tz-C12-POM samples (Figure 3b) were drastically different from those of Tz-C12 samples (Figure 3a). We also studied blank samples to check that the Tz-C12 sample immersed in pure acetonitrile, or the TSB-C12 sample (highly diluted solution of TSB molecules in toluene drop-casted on HOPG) immersed in a H3[PMo12O40] solution did not display those homogeneous films. The presence of the Tz-C12 sublayer is thus crucial, but also its long-range periodic organization. Indeed, we also studied a sample in which the layer of TzC12 was formed with a ten times more diluted solution (around 5.10-6 M in toluene). STM images showed that the substrate was not totally covered by the Tz-C12 molecules that appeared partially disorganized. FESEM and AFM images of this sample after immersion in a POM solution, exactly in the same conditions as described above, showed thick spaced POMs islands rather than thin extended films, that probably grew on nucleation sites formed by the disorganized Tz-C12 sublayer (Figure S15).

The last crucial point was to visualize the POMs at the nanoscale, in order to check that i) they were really isolated from each other and ii) they followed the periodicity of the Tz-C12 sublayer. This task was challenging because of the technique used, the STM in air, where a huge electric field (several GV.m-1) is applied between the tip and the sample, which can induce an alteration in the arrangement of the highly-charged POMs on the surface.32 Nevertheless, we succeeded in several cases to image stable well-organized islands of assumed

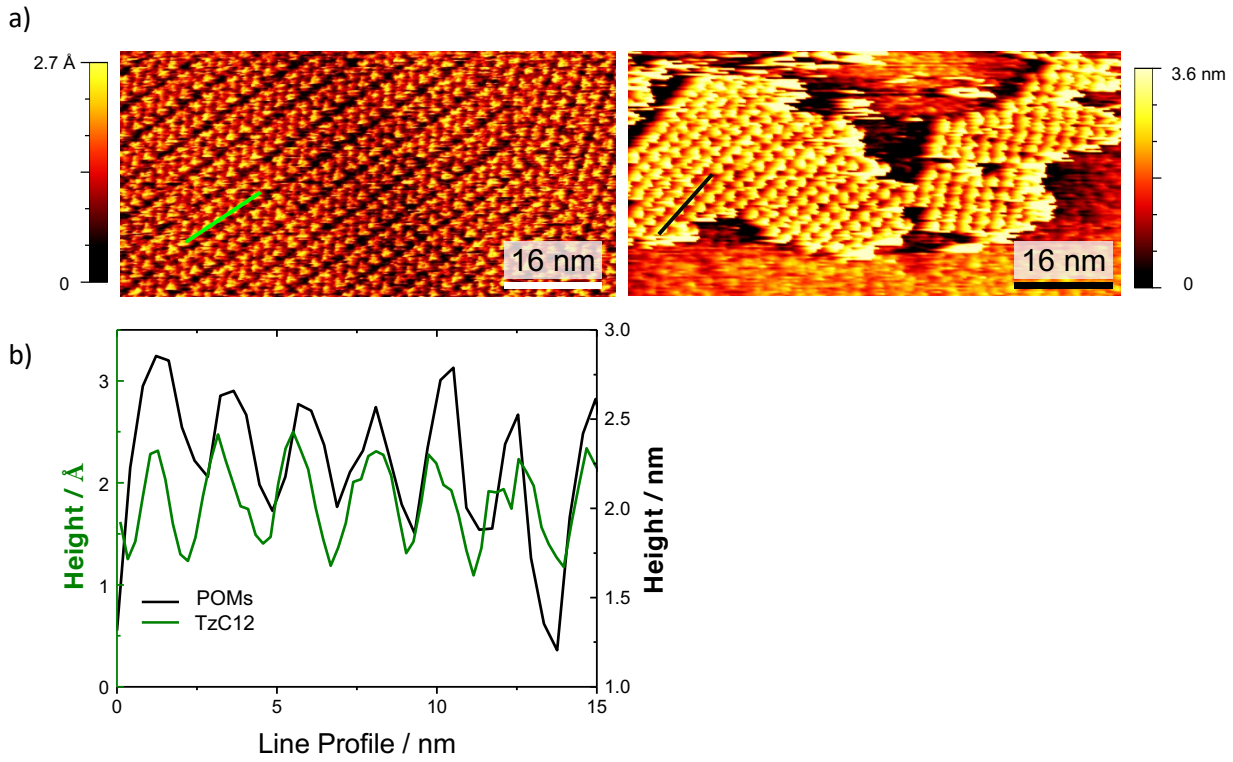

Figure 4. a) STM images of the Tz-C12 sample (from 5.10-5 M solution in toluene) showing the herringbones arrangements (left, I=15 pA, V=-1 V)) and the Tz-C12-POM sample (right, I=16 pA, V=-1.5 V)) b) apparent height profiles of the Tz-C12 and the Tz-C12-POM samples. The apparent height increases by one order of magnitude in the presence of the POMs.

POMs in which a clear POM-to-POM separation is around 1 nm (Figure 4). Moreover, the POMs showed periodicity of 2 nm, corresponding to inter-triazine distance in the underlying Tz-C12 assembly (Figure 4b and Figure S8). It is worth noting here that those images are clearly different from STM images of bare HOPG and that a Tz-C12 sample immersed in a solution of acidified acetonitrile (with HCl and without POMs) showed a homogeneous arrangement of the Tz-C12 (Figure S13). In the STM image of Tz-C12-POM sample (Figure 4a), the blurred contours of the islands correspond to the less stable molecules at the edges that probably moved under the STM tip. Also, in two images recorded one after the other, one can observe that some POMs have disappeared from the image, proving the strong irreversible interaction between the tip and the POMs (Figure S14).

In this study we demonstrate for the first time the periodical organization of individualized polyoxometalates. We used two classical methods in an original combination: electrostatic deposition of the POMs on organic self-assembled molecules usually used for their nanoporous 2D structure. The characterizations in solution and on the surface at various scales allowed to prove the acidification of the Tz-C12 self-assembled molecule by the H3[PMo12O40], the deposition of the POMs on the substrate as ultra-thin films over micrometric distances and their periodical organization at the molecular scale, with their individualization ensured by the observed 1nm POM-to-POM spacing. Local techniques of spectroscopy, such as nanoscale infrared spectroscopy, will be performed to shed more light on the chemical composition and structure of the self-assembled moieties. This study paves the

way for the deposition of numerous clusters and oxo-clusters exploiting a new mode of interaction with the underlying 2D self-assembled molecules.

Author Contributions

J.S. did the experiments (Tz-C12 synthesis, POMs deposition, NMR and UV-vis characterization, STM and AFM characterization), supported by M.M. and J.P.C., and participated to the conception of the project. J.C.P. performed DFT calculations. D.M. performed FESEM and EDS characterizations. A.M. performed XPS characterization and supervised XPS analysis. R.M. supervised NMR analysis and performed supplementary characterization not shown here. A.P. and G.I. supervised molecular synthesis. D.K. and I.A. supervised STM experiments and participated in the overall development of the project. FV conceived and supervised the project. F.V. wrote the manuscript with the contribution from all authors.

Conflicts of interest

There are no conflicts to declare.

Acknowledgments

We acknowledge support of the Ville de Paris (grant Emergence 2019 DAE 81). We thank the MS3U platform of the Fédération de chimie moléculaire Paris Centre FR 2769 for the MS measurements. We also thank Sorbonne Université, CNRS and Region Ile de France for the funding of FESEM and EDS equipment.

Notes and references

1 M. Glöß, R. Pütt, M. Moors, E. Kentzinger, S. Karthäuser and K. Yu. Monakhov, Adv Materials Inter, 2022, 9, 2200461.

2 F. Yang, M. Moors, D. A. Hoang, S. Schmitz, M. Rohdenburg, H. Knorke, A. Charvat, X.-B. Wang, K. Yu. Monakhov and J. Warneke, ACS Appl. Nano Mater., 2022, 5, 14216–14220.

3 L. Poggini, E. Tancini, C. Danieli, A. L. Sorrentino, G. Serrano, A. Lunghi, L. Malavolti, G. Cucinotta, A. Barra, A. Juhin, M. Arrio, W. Li, E. Otero, P. Ohresser, L. Joly, J. P. Kappler, F. Totti, P. Sainctavit, A. Caneschi, R. Sessoli, A. Cornia and M. Mannini, Adv Materials Inter, 2021, 8, 2101182.

4 A. Benchohra, C. Méthivier, J. Landoulsi, D. Kreher and R. Lescouëzec, Chem. Commun., 2020, 56, 6587–6589.

5 A. Saywell, G. Magnano, C. J. Satterley, L. M. A. Perdigão, A. J. Britton, N. Taleb, M. del Carmen Giménez-López, N. R. Champness, J. N. O'Shea and P. H. Beton, Nat Commun, 2010, 1, 75.

6 G. Lovat, B. Choi, D. W. Paley, M. L. Steigerwald, L. Venkataraman and X. Roy, Nature Nanotech, 2017, 12, 1050–1054.

7 L. Vergnani, A.-L. Barra, P. Neugebauer, M. J. Rodriguez-Douton, R. Sessoli, L. Sorace, W. Wernsdorfer and A. Cornia, Chem. Eur. J., 2012, 18, 3390–3398.

8 L. Llanos and D. Aravena, Journal of Magnetism and Magnetic Materials, 2019, 489, 165456.

9 C. Kato, R. Machida, R. Maruyama, R. Tsunashima, X.-M. Ren, M. Kurmoo, K. Inoue and S. Nishihara, Angew. Chem. Int. Ed., 2018, 57, 13429–13432.

10 J. P. Dela Cruz Calupitan, O. Galangau, O. Guillermet, R. Coratger, T. Nakashima, G. Rapenne and T. Kawai, Eur. J. Org. Chem., 2017, 17, 2451–2461.

11 X. Lu, M. Grobis, K. H. Khoo, S. G. Louie and M. F. Crommie, Phys. Rev. B, 2004, 70, 115418.

12 O. Linnenberg, M. Moors, A. Notario-Estévez, X. López, C. de Graaf, S. Peter, C. Baeumer, R. Waser and K. Yu. Monakhov, Journal of the American Chemical Society, 2018, 140, 16635–16640.

13 M. Mannini, P. Sainctavit, R. Sessoli, C. Cartier dit Moulin, F. Pineider, M.-A. Arrio, A. Cornia and D. Gatteschi, Chem. Eur. J., 2008, 14, 7530–7535.

14 T. Miyamachi, M. Gruber, V. Davesne, M. Bowen, S. Boukari, L. Joly, F. Scheurer, G. Rogez, T. K. Yamada, P. Ohresser, E. Beaurepaire and W. Wulfhekel, Nat Commun, 2012, 3, 938.

15 L. Zhang, Y. Tong, M. Kelai, A. Bellec, J. Lagoute, C. Chacon, Y. Girard, S. Rousset, M. Boillot, E. Rivière, T. Mallah, E. Otero, M. Arrio, P. Sainctavit and V. Repain, Angew. Chem. Int. Ed., 2020, 59, 13341–13346.

16 J. P. D. C. Calupitan, O. Guillermet, O. Galangau, M. Yengui, J. Echeverría, X. Bouju, T. Nakashima, G. Rapenne, R. Coratger and T. Kawai, J. Phys. Chem. C, 2018, 122, 5978–5991.

17 J. J. Baldoví, S. Cardona-Serra, A. Gaita-Ariño and E. Coronado, in Advances in Inorganic Chemistry, Elsevier, 2017, vol. 69, pp. 213–249.

18 C. Busche, L. Vilà-Nadal, J. Yan, H. N. Miras, D.-L. Long, V. P. Georgiev, A. Asenov, R. H. Pedersen, N. Gadegaard, M. M. Mirza, D. J. Paul, J. M. Poblet and L. Cronin, Nature, 2014, 515, 545–549.

19 X. Chen, P. Huang, X. Zhu, S. Zhuang, H. Zhu, J. Fu, A. S. Nissimagoudar, W. Li, X. Zhang, L. Zhou, Y. Wang, Z. Lv, Y. Zhou and S.-T. Han, Nanoscale Horizons, 2019, 4, 697-704

20 C. Huez, D. Guérin, S. Lenfant, F. Volatron, M. Calame, M. L. Perrin, A. Proust and D. Vuillaume, Nanoscale, 2022, 14, 13790–13800.

21 C. Wu, X. Qiao, C. M. Robertson, S. J. Higgins, C. Cai, R. J. Nichols and A. Vezzoli, Angew. Chem. Int. Ed., 2020, 59, 12029–12034.

22 X. Yi, N. V. Izarova, M. Stuckart, D. Guérin, L. Thomas, S. Lenfant, D. Vuillaume, J. van Leusen, T. Duchoň, S. Nemšák, S. D. 0M. Bourone, S. Schmitz and P. Kögerler, Journal of the American Chemical Society, 2017, 139, 14501–14510.

23 A. Balliou, M. Bouroushian, A. M. Douvas, G. Skoulatakis, S. Kennou and N. Glezos, Nanotechnology, 2018, 29, 275204.

24 M. Laurans, K. Trinh, K. Dalla Francesca, G. Izzet, S. Alves, E. Derat, V. Humblot, O. Pluchery, D. Vuillaume, S. Lenfant, F. Volatron and A. Proust, ACS Appl. Mater. Interfaces, 2020, 12, 48109–48123.

25 S. S. Amin, J. M. Cameron, R. B. Cousins, J. Wrigley, L. Liirò-Peluso, V. Sans, D. A. Walsh and G. N. Newton, Inorg. Chem. Front., 2022, 9, 1777–1784.

26 L. Yue, S. Wang, D. Zhou, H. Zhang, B. Li and L. Wu, Nat Commun, 2016, 7, 10742.

27 X.-S. Hou, G.-L. Zhu, L.-J. Ren, Z.-H. Huang, R.-B. Zhang, G. Ungar, L.-T. Yan and W. Wang, J. Am. Chem. Soc., 2018, 140, 1805–1811.

28 S. Sherif, G. Rubio-Bollinger, E. Pinilla-Cienfuegos, E. Coronado, J. C. Cuevas and N. Agraït, Nanotechnology, 2015, 26, 291001.

29 J. de Bruijckere, P. Gehring, M. Palacios-Corella, M. Clemente-León, E. Coronado, J. Paaske, P. Hedegård and H. S. J. van der Zant, Phys. Rev. Lett., 2019, 122, 197701.

30 D. Bonifazi, S. Mohnani and A. Llanes-Pallas, Chem. Eur. J., 2009, 15, 7004–7025.

31 L. Sosa-Vargas, E. Kim and A.-J. Attias, Mater. Horiz., 2017, 4, 570–583.

32 Q. Fernez, S. Moradmand, M. Mattera, W. Djampa-Tapi, C. Fiorini-Debuisschert, F. Charra, D. Kreher, F. Mathevet, I. Arfaoui and L. S. Vargas, J. Mater. Chem. C, 2022, 10, 13981–13988.

33 J. Zhang, S. Chang, B. H. R. Suryanto, C. Gong, X. Zeng, C. Zhao, Q. Zeng and J. Xie, Inorganic Chemistry, 2016, 55, 5585–5591.

34 A. Lombana, C. Rinfray, F. Volatron, G. Izzet, N. Battaglini, S. Alves, P. Decorse, P. Lang and A. Proust, J. Phys. Chem. C, 2016, 120, 2837–2845.

35 G. Schull, L. Douillard, C. Fiorini-Debuisschert, F. Charra, F. Mathevet, D. Kreher and A.-J. Attias, Nano Letters, 2006, 6, 1360–1363.

36 K. Dalla Francesca, S. Lenfant, M. Laurans, F. Volatron, G. Izzet, V. Humblot, C. Methivier, D. Guerin, A. Proust and D. Vuillaume, Nanoscale, 2019, 11, 1863–1878.

37 A. Balliou, G. Papadimitropoulos, G. Skoulatakis, S. Kennou, D. Davazoglou, S. Gardelis and N. Glezos, ACS Applied Materials & Interfaces, 2016, 8, 7212–7220.

38 B. Kim, C. Cho, I. Arfaoui, C. Paris, C. Petit, T. Le Bahers, E. Kim and A.-J. Attias, Mater. Horiz., 2020, 7, 2741–2748.

39 S. Le Liepvre, P. Du, D. Kreher, F. Mathevet, A.-J. Attias, C. Fiorini-Debuisschert, L. Douillard and F. Charra, ACS Photonics, 2016, 3, 2291–2296.

40 P. Du, D. Kreher, F. Mathevet, P. Maldivi, F. Charra and A.-J. Attias, ChemPhysChem, 2015, 16, 3774–3778.

41 F. C. Schaefer and P. A. Grace, Journal of organic chemistry, 1961, 2778.

42 H. Meier, H. C. Holst and A. Oehlhof, Eur. J. Org. Chem., 2003, 2003, 4173–4180.

43 A. Bellec, C. Arrigoni, G. Schull, L. Douillard, C. Fiorini-Debuisschert, F. Mathevet, D. Kreher, A.-J. Attias and F. Charra, The Journal of Chemical Physics, 2011, 134, 124702.

44 X. Song, Y. Ma, C. Wang, P. M. Dietrich, W. E. S. Unger and Y. Luo, J. Phys. Chem. C, 2012, 116, 12649–12654.